University of Anbar

Anbar Journal of Engineering Science©

journal homepage: **https://ajes.uoanbar.edu.iq/**

Direct Algorithm for Computation of Inverse Real Fast Fourier Transform (IRDFT)

Sukaina K. Saliha, Mounir T. Hamoodb

a,bDepartment of the Electrical Engineering, College of Engineering, University of Tikrit, Iraq

ABSTRACT

This paper proposes an efficient algorithm for fast computation of the inverse real-valued discrete Fourier transform (IRDFT) using the decimation in frequency (DIF) approach. The proposed algorithm represents a direct method with a new implementation for fast computing of IRDFT. The algorithm derivation is based on the basic principles of the Cooley-Tukey algorithm with the divide and conquer approach and utilizes the advantage of conjugate symmetric property for the discrete Fourier transform (DFT) to remove all redundancies that appear when DFT deals with real data. The analyses of the proposed algorithm have shown that the arithmetic number has reached a minimum, therefore the structure of the developed algorithm possesses the desired properties such as regularity, simplicity, and in-place computation. The arithmetic complexity of this algorithm has been compared with the inverse FFT algorithm, and it was found that it needs the least number of multiplications and additions. The validity of the developed algorithm has been verified by reducing the peak-to-average power ratio PAPR in optical-OFDM systems compared with complex FFT. The simulation using MATLAB(R2021a) findings show that the RFFT O-OFDM system reduces PAPR more efficiently than the FFT O-OFDM system. The PAPR exhibits a reduction of approximately 2.4 to 2.75 dB when evaluated at a probability of occurrence of 10^{-1} in the complementary cumulative distribution function (CCDF) plot.

1. Introduction

Fast Fourier Transform (FFT) is a method that is highly efficient for computing the DFT, and it has a very important role in digital signal processing applications like speech [1], image [2], spectral estimation [3], radar, and digital communication. FFT commonly operates on complex signals, and the efficient design for the complex FFT (CFFT) has been studied widely [4-6]. The FFT spectrum is symmetric when real-valued signals are used as

* Corresponding author: Sukaina K. Salih; sukina.k.saleh44346@st.tu.edu.iq ; +964-07707520779

input samples, which means that just one-half of the normal number of operations are required. The calculations of the FFT using the samples from the real input is not optimized for them (RFFT). Most of the physical signals are real [7,8]. The FFT of real-valued data is used in many different types of applications, including voice, video, and image processing [9], and optical wireless communication (OWC), Therefore, it is necessary to use algorithms that specifically deal only with real signals [10,11]. The architecture of the RFFT is presented in many designs and applications in the literature [12-14]. Burrus et al in [15] produced decimation in time RFFT algorithm by using symmetric conjugate, it has proved challenging to do the same design for decimation in frequency. In [16] Lao and Parhi presented a real-valued algorithm (RFFT) by using the canonic property to design RFFT and this algorithm is suitable. The canonic RFFT approach requires the least number of butterfly operation and its lead to higher regularity architectures that are decreased complexity of the hardware

In Dorota Majorkowska-Mech and Aleksandr Cariow [17] present a set of algorithms for real short-length RDFTs for N from 3 to 9, with corresponding signal flow graphs. The algorithms are written in matrix-vector notation, factorizing RDFT matrices and sparse matrices to reduce arithmetic operations. Although not repeating for different input vector lengths, the solutions are original and may be helpful.

The RFFT computation efficiency has drawn a lot of attention and focus for the past few years because of its multiple uses in different applications, Due to this feature a novel algorithm is presented in this paper to compute the DIF of IRFFT by removing explicit redundancies and computing the arithmetic complexity for this technique, as well as investigating the effectiveness of the suggested algorithm in an optical-OFDM system to prove that it can reduce PAPR compared with the complex DFT.

The outline of this paper is organized as follows: Section 2 definition real discrete Fourier transform (RDFT) and analysis of the proposed radix-2 IRFFT DIF algorithm. Section 3 presents the O-OFDM system. Section 4's result and discussion. Paper conclusion in section 5.

2. Proposed Algorithm

The definition of RDFT is based on the DFT, where the DFT for the sequence c(n) could be shown in mathematical form [18] as:

$$C(k) = \sum_{n=0}^{L-1} c(n) \, W_L^{nk} \qquad k = 0,1,2,...L-1 \qquad (1)$$

Where $W_L = e^{j2\pi L}$, L is the length of sequence c(n). The forward of RDFT can also defined as [17]:

$$R(k) = \sum_{n=0}^{L-1} r(n) \, \left(\cos \tfrac{2\pi nk}{L} + \theta(k)\right) \qquad (2)$$

Bothe R(k) and r(n) is reals, k=0,1,...L-1.

Where

$$\theta(k) = \begin{cases} 0 & 0 \le k \le L_2 \\ \dfrac{\pi}{2} & L_2 \langle k \le L-1 \end{cases} \qquad (3)$$

L2 is half length L. The Inverse of RDFT is written [17] as:

$$r(n) = \frac{2}{L} \sum_{k=0}^{L-1} R(k)v(n) \cos\left(\frac{2\pi nk}{L} + \theta(k)\right) \qquad (4)$$

Where

$$v(n) = \begin{cases} \dfrac{1}{2} & n = 0, L_2 \\ 1 & otherwise \end{cases} \qquad (5)$$

The derivation of the radix-2 IRFFT is implemented in DIF instead of the DIT approach because the redundancies are more straightforward and more effective in DIF therefore, the DIF approach is a natural choice for the derivation of the IRFFT.

From the definition of IRDFT in Eq (4) for length L, where L is a power 2, and by dividing the length to half:

$$r(n) = \sum_{k=0}^{L_2-1} R(k)\cos\left(\frac{2\pi nk}{L} + \theta(k)\right)$$
$$+ \sum_{k=0}^{L_2-1} R(k+L_2)\cos\left(\frac{2\pi n(k+L_2)}{L} + \theta(k+L_2)\right)$$
$$(6)$$

The first summation in Eq (6) represent IRFFT where the second summation can be Simplification through employment of the next trigonometric identities:

$$\cos(x+y) = \cos(x)\cos(y) - \sin(x)\sin(y)$$

And write as:

$$= \sum_{k=0}^{L_2-1} (-1)^n R(k+L_2)\cos\left(\frac{2\pi nk}{L} + \theta(k+L_2)\right) \quad (7)$$

$$= \sum_{k=0}^{L_2-1} (-1)^n R(k+L_2)\sin\left(\frac{2\pi nk}{L} + \theta(k)\right) \quad (8)$$

Eq (8) is compensated in Equation (6) that yields to:

$$r(n) = \sum_{k=0}^{L_2-1} R(k) + (-1)^n R(k-L_2)\cos\left(\frac{2\pi nk}{L} + \theta(k)\right) \quad (9)$$

Then we divide length L by the odd and even parts, and after some manipulation, we obtain:

$$r(2n) = \sum_{k=0}^{L_2-1}\left\{\left[R(k) + R(L_2-k)\right]\cos\left(\frac{2\pi nk}{L_2} + \theta(k)\right)\right\}$$
$$+ \sum_{k=0}^{L_2-1}\left\{\left[R(L-k) + R(L_2+k)\right]\cos\left(\frac{2\pi nk}{L_2} + \theta(k)\right)\right\}\cos\left(\frac{\pi k}{L}\right)$$
$$- \sum_{k=0}^{L_2-1}\left\{\left[X(k) - X(L_2-k\right]\cos\left(\frac{2\pi nk}{L_2} + \theta(k)\right)\right\}\sin\left(\frac{\pi k}{L}\right)$$
$$(10)$$

In the same manner, we can find the negative decompositions of the proposed algorithm:

$$r(L-2n-1) = \sum_{k=0}^{L_2-1}\left[R(L-k) - R(L_2+k)\right]\cos\left(\frac{2\pi nk}{L_2} + \theta(k)\right)$$

$$+ \sum_{k=0}^{L_2-1}\left\{\left[R(k) - R(L_2-k)\right]\cos\left(\frac{2\pi nk}{L_2} + \theta(k)\right)\right\}\cos\left(\frac{\pi k}{L}\right)$$
$$+ \sum_{k=0}^{L_2-1}\left\{\left[R(L_2+k) + R(L-k)\right]\cos\left(\frac{2\pi nk}{L_2} + \theta(k)\right)\right\}\sin\left(\frac{\pi k}{L}\right)$$

$$(11)$$

From the decomposition Eqs (10) and (11) can be draw the butterfly of the suggested IRFFT-DIF algorithm as shown in Figure 1.
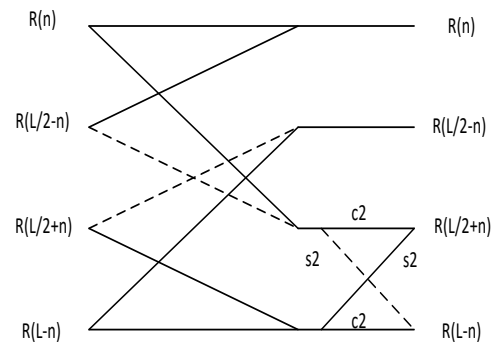

Figure 1. Inverse real-valued Butterfly, soild lines for additions and dotted lines for subtraction.

2.1 Complexity of IRFFT Algorithm

In this part of the article, we will go over the computation for DIF IRFFT. From the flow graph for L=16 DIF IRFFT displayed in Figure 2, observe that the proposed algorithm is need (Log2 L) stages of butterfly for length L.

The redundancies of DIF IRFFT that result from the conjugate symmetric are removed, which reduces the number of computations. The first and second stages represent a special case where it requires (L-4) additions and doesn't have multiplication. The third stage has L number of additions and number of multiplications. Each butterfly in all stages has two reductions, except in the first stage, where the reductions in the last stage take place at points L/4 and 3L/4. From the structure of the proposed algorithm, we analyzed and calculated how many real multiplications $M_R(L)$ there are and real additions $A_R(L)$ as follows:

$$M_R(L) = L(Log_2 L - 2) - (L-4) \quad (12)$$

$$A_R(L) = \frac{3L}{2}(Log_2 L - 2) + \frac{3L}{2} - (L - 4) \qquad (13)$$

Simplifications of (12) and (13) yields:

$$M_R(L) = L(Log_2 L) - 3L + 4 \qquad (14)$$

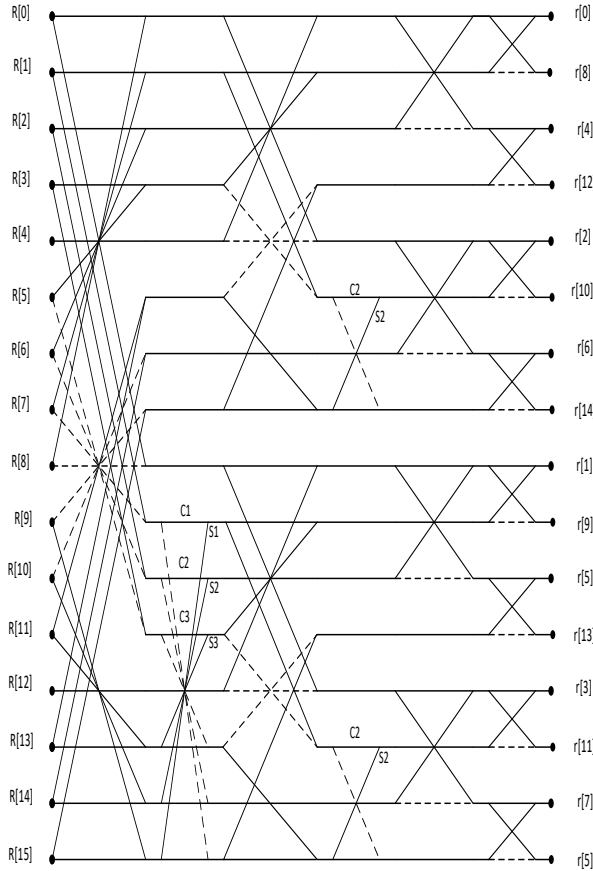$$A_R(L) = \frac{3L}{2}Log_2 L - \frac{5L}{2} + 4 \qquad (15)$$

Figure 2. Radix-2 IRFFT signal flow graph when the length L= 16, where $si = \sin\frac{2\pi i}{L}$ and $ci = \cos\frac{2\pi i}{L}$ respectively,

While the complexity of IFFT for real data is found as [19]:

$$M_C(L) = 2L(Log_2 L) \qquad (16)$$

$$A_C(L) = 3L(Log_2 L) \qquad (17)$$

Where $M_C(L)$ numbere of multiplications and $A_C(L)$ number of additions.

3. Optical OFDM System

Orthogonal Frequency Division Multiplexing (OFDM) is one of the types of communication technologies that represent multi-carrier modulation, as it is used very widely because of the advantages it offers, the most important of which are immunity to frequency fading and the ability to prevent Inter-Symbol Interference (ISI) across subcarriers due to the orthogonality properties [20].

OFDM technology can be used for the optical spectrum instead of the radio frequency (RF) spectrum. It is known that optical wireless communication (OWC) is one of the most modern, important and pioneering systems in the world of Wireless Communications (WC) technologies that depend on real signals. The growing need for wireless capacity in the traditional radio frequency (FR) band has drawn attention to optical communications (OC) due to optical spectrum advantages [21]. The OWC depended on the Intensity Modulation/Direct Detection (IM/DD) techniques. In IM/DD the signal should be positive and real-valued, which requires modifications to traditional communication algorithms. Where depends on Visible Light Communication (VLC) as a medium for indoor wireless information transmission. In VLC systems, the most common modulation strategy is IM, in which the electrical impulses are intensity modulated by the LEDs, and this demands a real and non-negative signal. In Optical OFDM (O-OFDM) to make the signal positive (a unipolar signal) there are several methods, the most widely used are Direct Current biased Optical OFDM (DCO-OFDM) and Asymmetrically Clipped Optical OFDM (ACO-OFDM) [22].

In general, FFT and IFFT represent a core for the transmitter and receiver, which deal with complex signals. In VLC, the signal must be real and positive due to the use of the IM/DD method. To obtain a real signal, we resort to placing a Hermitian Symmetric (HS) block before IFFT. Below the equation of HS [23]:

$$C(k) = C^*(2L - k) \qquad (18)$$

Where $C(0) = C(L) = 0$, that means the length of the input signal L becomes 2L to achieve HS. The input

of IFFT using HS can be expressed:

$$C(k) = \left[0, C_1, C_2, ..., C_L, 0, C_L^*, C_{L-1}^*, ..., C_1^* \right] \qquad (19)$$

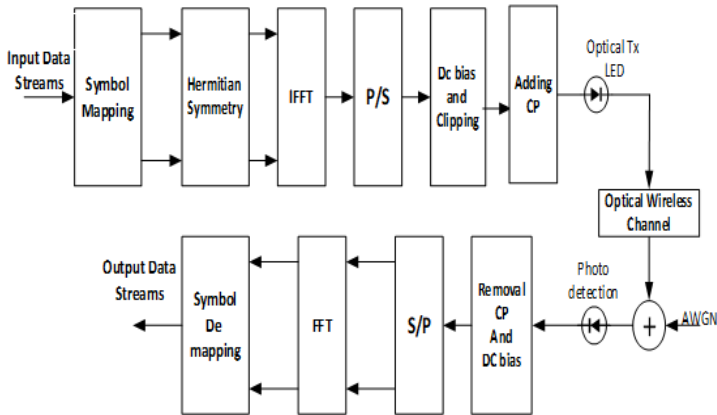Figure 3 shows the traditional method for O-OFDM by using FFT.

Figure 3. DCO-OFDM system [22]

The time domain of the DCO-OFDM system will be created after the IFFT process as follows:

$$c(n)_{O-OFDM} = \frac{1}{2L} \sum_{k=0}^{2L-1} C(k) \, e^{2\pi nk/L} \qquad (20)$$

Light Emitting Diodes (LED) and Laser diode (LD) employed to transform the electrical signal to optical signal.

Despite this method having many benefits, O-OFDM has a number of disadvantages. The peak-to-average power ratio (PAPR) is one of O- OFDM's most significant problems which is [24] :

$$PAPR = \frac{\max \left\{ |c(n)|^2 \right\}}{E \left\{ |c(n)|^2 \right\}} \qquad (21)$$

Where c(n) is O-OFDM signal and E represents the average value. When the PAPR is high, the nonlinear property of LED will have a significant effect on the operating efficiency of VLC systems that make use of IM/DD modulation in conjunction with OFDM. Given that the signal has a high PAPR and a Gaussian distribution, OFDM needs a large linear operating dynamic range. Due to the clipping of the peak amplitudes of the OFDM signal as a result of the high PAPR, additional clipping noise is

produced for a system with a constrained linear dynamic range. Therefore, it is necessary to reduce the PAPR to maintain efficient system performance [25].

The proposed RFFT may be considered one of the possible solutions for the PAPR problem in O-OFDM systems due to its attractive features.

In the case of employing the IRFFT for the transmitter of O-OFDM, we do not need to use HS because it deals with real input and output, which means it maintains the same length of the input data. Figure 4 shows the transmitter device of O-OFDM using IRFFT.
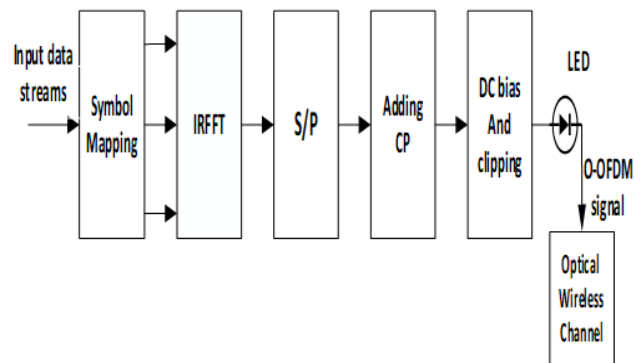

Figure 4. The transmitter of O-OFDM using IRFFT.

4. Result and Discussion

In this section, we show the results of comparing the proposed algorithm with the traditional method IFFT for real vauled in terms of computational complexity by using the Eqs (14,15,16,17)

Figure 5 shows the wide difference between IRFFT and IFFT for real data in the number of operations, where the IFFT requires double the quantity of multiplications and additions.
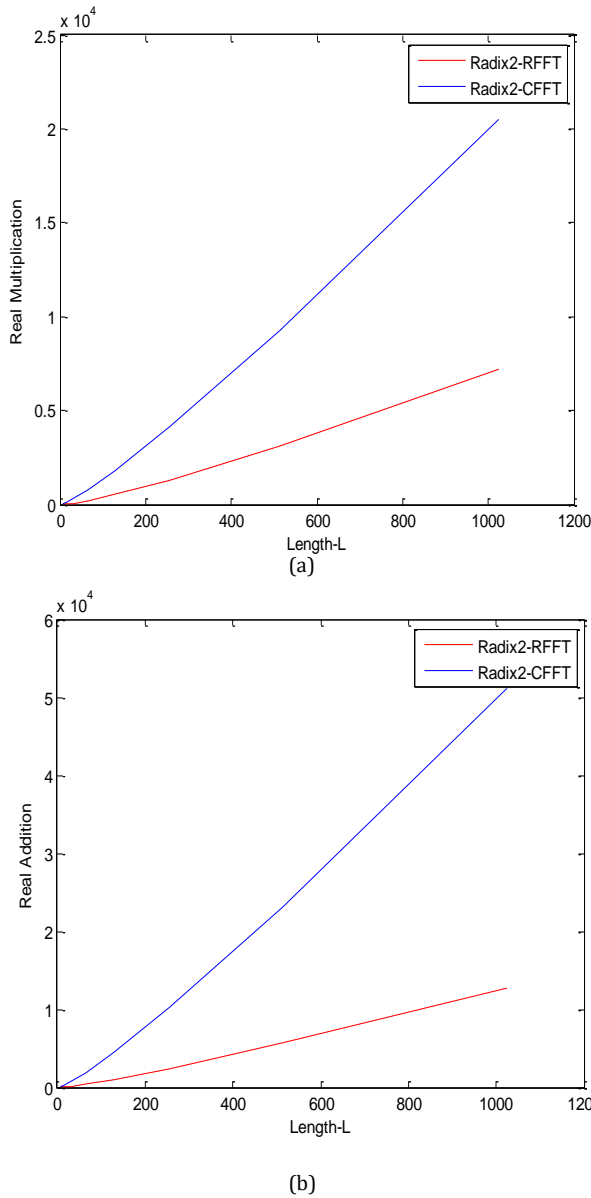
(a)

(b)

Figure 5. The Arithmetic Operations for RFFT and CDFT: (a)Real Multiplications. (b)Real Additions.

The performance efficiency of the proposed algorithm IRFFT was evaluated by employing it in the OFDM indoor visible light communication (VLC) scheme will be conducted with a focus on the decreased PAPR.

Notably, the IRFFT of O-OFDM can be used with complex modulating forms such as QPSK and 16-QAM as well as real modulating forms such as PAM and BPSK, due to the fact that the IRFFT algorithm is applied twice for complex modulating and once for real modulatin.

Figures 6 and 7 illustrates that the suggested RFFT-O-OFDM system exhibits a reduction in PAPR when compared to the O-OFDM indoor VLC systems that are based on FFT at the CCDF of 10^{-1} in QAM modulation, the proposed RFFT-O-OFDM system achieves PAPR reductions of around 2.5 dB and 2.4 dB for 256-point IRFFT and 1024-point IRFFT, respectively.
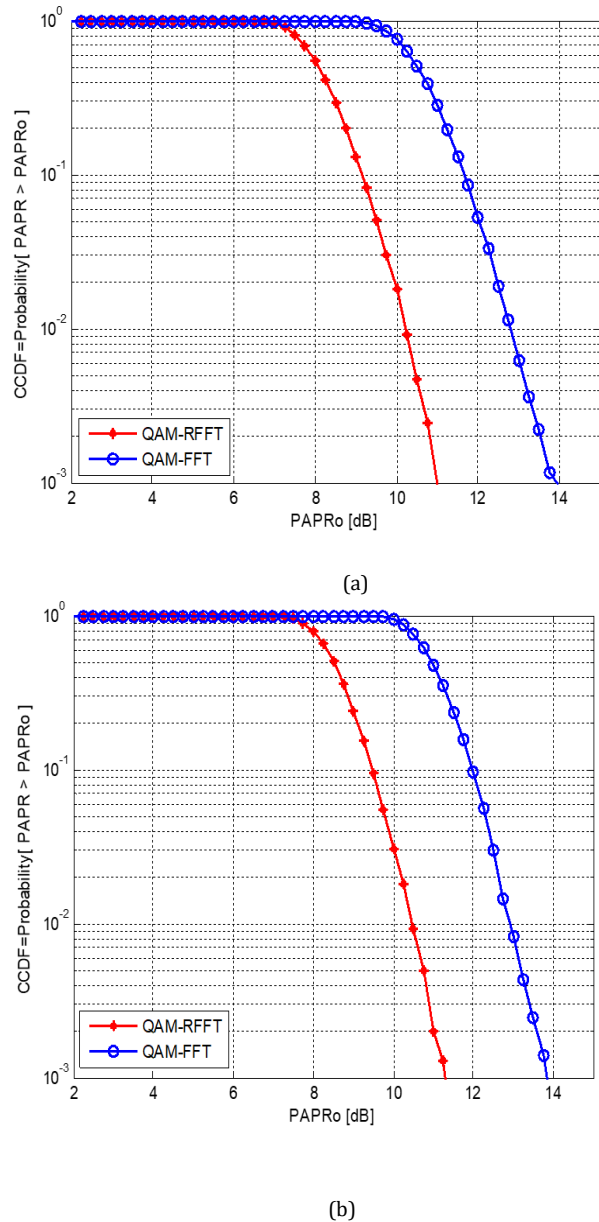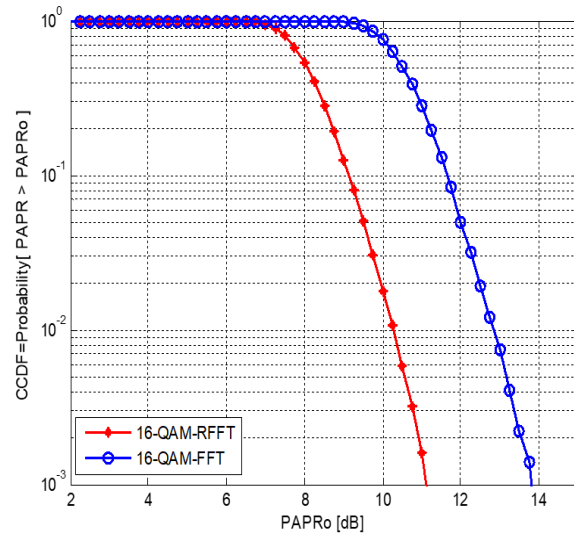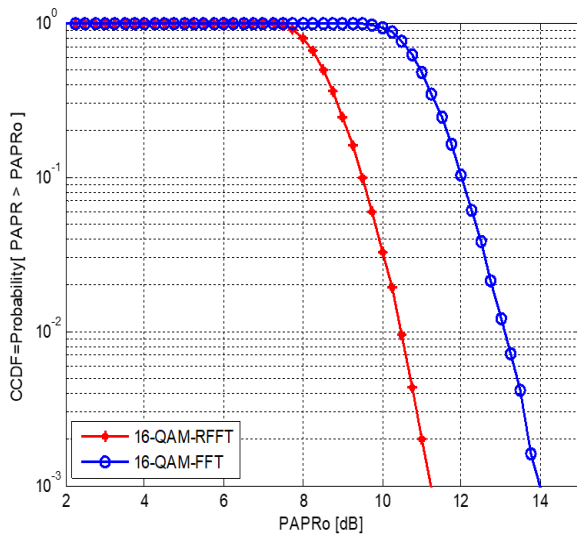

(a)

(b)

Figure 6. CCDF of the proposed IRFFT O-OFDM and IFFT O-OFDM for the QAM modulation, for (a) L=256, (b) L =1024.

(a)

(b)

Figure 7. CCDF of the proposed IRFFT O-OFDM and IFFT O-OFDM for the 16- QAM modulation, for (a) L=256, (b) L =1024

The results obtained from reducing PAPR for various orders of QAM modulations and sizes of O-OFDM are summarized in Table 1.

Table 1. PAPR performance

The NO. of Subcarriers	PAPR Reduction (QAM) in dB	PAPR Reduction (16QAM) in dB
256	∼ 2.5	∼ 2.75
1024	∼ 2.4	∼ 2.45

Table 2 displays the parameters of the suggested RFFT O-OFDM system versus the conventional O-OFDM system [26].

Table 2. Parameters of the proposed system

Parameters	Value
Transform Size	1024
Cyckic Prefix (CP) Length	256
Sample Time	88ns
Number of Transmitted Frames	10^4

5. Conclusion

A unique IRFFT decimation in frequency algorithm has been presented. Applying this algorithm (IRFFT) shows that the redundancies at every stage are efficiently removed, in contrast to the decimation in time (DIT) approach. The structure of the developed algorithm has low arithmetic complexity, up to half the operations compared to the conventional IFFT. Furthermore, the simplicity of the developed algorithm helps us maintain the regularity of the butterfly structure. The suggested algorithm was applied in O-OFDM based on VLC, where the simulation took two modulation orders, including QAM, and 16QAM, and different information data length was set at L = 256 and L = 1024.
Results of the simulation proved that using the proposed IRFFT algorithm, the reduction was noticeable in the gain of the PAPR at a CCDF plot compared with the conventional FFT O-OFDM system.

Refrences

[1] D. Takahashi and D. Takahashi, "Fast fourier transform," *Fast Fourier Transform Algorithms for Parallel Computers, vol. 2, 2019,* pp. 5-13.

[2] G. Plewa, "A new form of discrete real Fourier transform and its potential applications," Ann Math Phys, vol. 2, no. 5, pp. 160-166, Nov. 2022, doi: 10.17352/amp.000060

[3]   M. Khayyeri and K. Mohammadi, "Cooperative wideband spectrum sensing in cognitive radio based on sparse real-valued fast fourier transform," *IET Communications,* vol. 14, no. 8, pp. 1340-1348, May. 2020, doi:10.1049/iet-com.2018.5930

[4]   O. Roienko, V. Lukin, V. Oliinyk, I. Djurović, and M. Simeunović, "An Overview of the Adaptive Robust DFT and It's Applications," *Technological Innovation in Engineering Research, Vol. 4,* pp. 68-89, 2022, doi:10.9734/bpi/tier/v4/6314F.

[5]   K. J. Jones, "A Comparison of Two Recent Approaches, Exploiting Pipelined FFT and Memory-Based FHT Architectures, for Resource-Efficient Parallel Computation of Real-Data DFT,", June. 2023 doi: 10.21203/rs.3.rs-3092888/v1

[6]   E. Rajaby and S. M. Sayedi, "A structured review of sparse fast Fourier transform algorithms," *Digital Signal Processing,* vol. 123, p. 103403, Apr.2022, doi:10.1016/j.dsp.2022.103403.

[7]   K. J. Jones, "Design for Resource-Efficient Parallel Solution to Real-Data Sparse FFT," Jul. 2023, doi:10.21203/rs.3.rs-3133148/v1

[8]   A. A. Naoghare and A. V. Sakhare, "Review on FFT architecture for real valued signals using Radix 25 algorithm," 2015 International Conference on Pervasive Computing (ICPC), Pune, India, 2015, pp. 1-3, doi: 10.1109/PERVASIVE.2015.7087124.

[9]   B. K. Mohanty and P. K. Meher, "Area–Delay–Energy Efficient VLSI Architecture for Scalable In-Place Computation of FFT on Real Data," in IEEE Transactions on Circuits and Systems I: Regular Papers, vol. 66, no. 3, pp. 1042-1050, Mar. 2019, doi: 10.1109/TCSI.2018.2873720.

[10]   D. A. Tsonev, "High speed energy efficient incoherent optical wireless communications," University of Edinburgh, 2015.

[11]   S. Park and D. Jeon, "A Modified Serial Commutator Architecture for Real-Valued Fast Fourier Transform," 2020 IEEE Workshop on Signal Processing Systems (SiPS), Coimbra, Portugal, 2020, pp. 1-6, doi: 10.1109/SiPS50750.2020.9195236.

[12]   C. Eleftheriadis and G. Karakonstantis, "Energy-Efficient Fast Fourier Transform for Real-Valued Applications," in IEEE Transactions on Circuits and Systems II: Express Briefs, vol. 69, no. 5, pp. 2458-2462, May. 2022, doi: 10.1109/TCSII.2022.3163280.

[13]   D. Takahashi, "An implementation of parallel 1-D real FFT on Intel Xeon Phi processors," in *International Conference on Computational Science and Its Applications*, 2017: Springer, pp. 401-410.

[14]   H. Sorensen, D. Jones, M. Heideman and C. Burrus, "Real-valued fast Fourier transform algorithms," in IEEE Transactions on Acoustics, Speech, and Signal Processing, vol. 35, no. 6, pp. 849-863, June. 1987, doi: 10.1109/TASSP.1987.1165220.

[15]   Y. Lao and K. K. Parhi, "Data-Canonic Real FFT Flow-Graphs for Composite Lengths," 2016 IEEE International Workshop on Signal Processing Systems (SiPS), Dallas, TX, USA, 2016, pp. 189-194, doi: 10.1109/SiPS.2016.41..

[16]   D. Majorkowska-Mech and A. Cariow, "Some FFT Algorithms for Small-Length Real-Valued Sequences," Applied Sciences, vol. 12, no. 9, p. 4700, May. 2022, doi:10.3390/app12094700

[17]   G. G. Kumar, S. K. Sahoo, and P. K. Meher, "50 years of FFT algorithms and applications," *Circuits, Systems, and Signal Processing,* vol. 38, pp. 5665-5698, May. 2019, doi:10.1007/s00034-019-01136-8

[18]   X. Zhang, Z. Babar, P. Petropoulos, H. Haas and L. Hanzo, "The Evolution of Optical OFDM," in IEEE Communications Surveys & Tutorials, vol. 23, no. 3, pp. 1430-1457, thirdquarter 2021, doi: 10.1109/COMST.2021.3065907

[19]   X. Huang, Q. Wang, S. Lu, R. Hao, S. Mei, and J. Liu, "Evaluating FFT-based Algorithms for Strided Convolutions on ARMv8 Architectures?," *ACM SIGMETRICS Performance Evaluation Review,* vol. 49, no. 3, pp. 28-29, Mar. 2022, doi:10.1145/3529113.3529122

[20] Z. Wang, Q. Wang, W. Huang, and Z. Xu, *Visible light communications: modulation and signal processing*. John Wiley & Sons, 2017.

[21] X. Deng, S. Mardanikorani, G. Zhou and J. -P. M. G. Linnartz, "DC-Bias for Optical OFDM in Visible Light Communications," in IEEE Access, vol. 7, pp. 98319-98330, Jul. 2019, doi: 10.1109/ACCESS.2019.2928944

[22] O. D. Saied, *Orthogonal frequency division multiplexing for indoor visible light communication links*. University of Northumbria at Newcastle (United Kingdom), 2018.

[23] K. Ramadan and M. S. Elbakry, "Performance Improvement for Optical OFDM Systems Using Symbol Time Compression," 2022, doi:10.21203/rs.3.rs-1725212/v1

[24] M. Mounir, M. I. Youssef, and A. M. Aboshosha, "Low-complexity selective mapping technique for PAPR reduction in downlink power domain OFDM-NOMA," *EURASIP Journal on Advances in Signal Processing,* vol. 2023, no. 1, p. 10, Jan. 2023, doi:10.1186/s13634-022-00968-y

[25] A. A. Abdulkafi, M. Y. Alias, Y. S. Hussein, N. Omar and M. K. B. Salleh, "PAPR reduction of DC biased optical OFDM using combined clipping and PTS techniques," 2017 IEEE 13th Malaysia International Conference on Communications (MICC), Johor Bahru, Malaysia, Nov. 2017, pp. 207-212, doi: 10.1109/MICC.2017.8311760.

[26] M. S. Ahmed, "OFDM base T-transform for wireless communication networks," Newcastle University, 2012.